

Postintubation Tracheal Stenosis Evaluated by Endobronchial Optical Coherence Tomography: A Canine Model Study

Zi-Qing Zhou^a Zhu-Quan Su^a Wan Sun^a Ming-Lu Zhong^b Yu Chen^a
Chang-Hao Zhong^a Huan-Jie Chen^a Shi-Yue Li^a

^aState Key Laboratory of Respiratory Disease, National Clinical Research Center for Respiratory Disease, Guangzhou Institute of Respiratory Health, The First Affiliated Hospital of Guangzhou Medical University, Guangzhou, China;

^bGuangzhou First People's Hospital, Guangzhou, China

Keywords

Optical coherence tomography · Postintubation tracheal stenosis · Airway morphology

Abstract

Background: The predictors and airway morphological changes during the development of postintubation tracheal stenosis (PITS) have not been well elucidated. **Objectives:** To elucidate the validation of endobronchial optical coherence tomography (EB-OCT) in assessing the airway morphological changes in PITS. **Methods:** We performed oral endotracheal intubation in 12 beagles to establish the PITS model. EB-OCT was performed respectively before modeling and on the 1st, 7th, and 12th day after extubation in 9 canines, and was conducted consecutively in 3 canines during the development of PITS. Histological findings and the thickness and gray-scale value of the tracheal wall assessed by EB-OCT measurements were analyzed and compared. **Results:** The tracheal wall edema, granulation tissue proliferation, cartilage destruction in PITS, and airway wall thickening detected by EB-OCT were in concordance with the histopathological measurements. The consecutive EB-OCT observation of the airway structure demonstrated the tracheal wall thickness

significantly increased from $344.41 \pm 44.19 \mu\text{m}$ before modeling to $796.67 \pm 49.75 \mu\text{m}$ on the 9th day after modeling ($p < 0.05$). The airway wall gray-scale values assessed by EB-OCT decreased from 111.19 ± 14.71 before modeling to 74.96 ± 4.08 on the 9th day after modeling ($p < 0.05$). The gray-scale value was negatively correlated with the airway wall thickness ($r = -0.945, p = 0.001$). **Conclusion:** The EB-OCT imaging, in concordance with the histopathological finding, was validated for assessing the airway morphological changes during the development of PITS. The EB-OCT evaluation of cartilage damage and gray-scale value measurement might help predict the development and prognosis of PITS.

© 2020 S. Karger AG, Basel

Introduction

Postintubation tracheal stenosis (PITS) is one of the most common causes of benign airway obstruction and is usually induced by excessive cuffed pressure, resulting in ischemic injury to the airway wall [1, 2]. Our previous

Drs. Zi-Qing Zhou, Zhu-Quan Su, and Wan Sun are co-first authors.

study [3] had introduced a canine model of tracheal stenosis induced by endotracheal intubation, indicating that proliferation of granulation tissue and ischemic necrosis of tracheal cartilage were found 2 weeks after extubation.

The development of interventional pulmonology and video-assisted thoracoscopic surgery has improved the therapeutic effect of PITS. Nevertheless, as the pathogenesis is not well elucidated, airway restenosis remains a challenge for the prognosis of PITS. Identifying the tracheal wall morphological changes after endotracheal intubation might help further understand the pathophysiological mechanisms of benign tracheal stenosis. Bronchoscopy is commonly used to identify the type, localization, and degree of tracheal stenosis [4], but confers limitation of inability to detect the airway wall structure. Computed tomography (CT) has been a useful modality to evaluate the airway morphology but lacks high-resolution display of luminal lesion and airway wall architecture [5]. Endobronchial optical coherence tomography (EB-OCT) is a novel imaging technology which provides a high-resolution image of the bronchial wall structure, revealing airway epithelium, basement membrane, lamina propria, and cartilage [6–8]. Hence, we hypothesized that EB-OCT might accurately measure the tracheal morphological changes during the development of PITS *in vivo*.

In the current study, we used EB-OCT to consecutively observe the morphological characteristics of the tracheal segment compressed by the endotracheal intubation cuff, and elucidate the EB-OCT evaluation on the changes of the tracheal wall structure secondary to endotracheal intubation with excessive cuffed pressure.

Method

Animal Objects

Twelve adult beagle dogs (aged 11–13 months, weight 10–13 kg) were provided by Guangzhou Bio Frontier Company. Nine of the 12 canines were averagely divided into 3 groups and respectively euthanized on the 1st, 7th, and 12th day after modeling to verify the concordance between EB-OCT and histological measurements. Moreover, the tracheal segment, that 3 cm beyond the compressed lesion was deemed as the normal airway, was assessed by EB-OCT measurement and histological examination as control for analysis and comparison. The other 3 canines received EB-OCT assessments daily to evaluate the airway wall morphological changes during the development of PITS.

Establishing the Animal Model of Tracheal Stenosis

The beagle model of PITS was established as described in our previous study [3]. Under general anesthesia, endotracheal intubation was performed under laryngoscopic guidance. Cuffed tubes with an internal diameter of 8.0 mm (Well Lead, Guangzhou, Chi-

na) were chosen for intubation. The depth of tube insertion was adjusted such that the top of the balloon was 3–4 cm below the glottis. The intra-cuff pressure was kept at 200 mm Hg, and the oral endotracheal intubation was maintained for 24 h.

EB-OCT Performance and Imaging Analysis

EB-OCT scanning was performed using the OCTICS Imaging (Guangzhou Winstar Medical Technology Company Limited, Guangzhou, China) system before and after modeling. The EB-OCT probe, 2.5 mm in outer diameter with automated rotating and rotary auto-pullback functions, was inserted under the guidance of a bronchoscope (B260F; Olympus, Tokyo, Japan). EB-OCT scanning was performed on the anterolateral and bilateral airway wall; thereafter, transcutaneous puncture with the sterile needle and nylon wire was conducted to accurately identify the tracheal segment compressed by an inflated intubation cuff. At least 3 reproducible OCT measurements were performed for each tracheal segment. The thickness and gray-scale value of the tracheal wall were obtained and measured by the OCTICS software system workstation.

Histological Analysis

Histological measurements of the excised tracheal segment in 9 canines were analyzed on the 1st, 7th, and 12th day after extubation, respectively. The tissue block was cut perpendicular to the long axis of the airway at the positioning segment, placed in an embedding box, and fixed in a 10% neutral formalin solution for routine continuous paraffin preparation. The slides were stained with H-E and observed by optical microscope (BX53; Olympus). The thickness of the airway wall, and the morphology of mucosa, cartilage, and granulation were analyzed.

Statistical Analysis

Statistical analysis was performed using SPSS version 20.0 software package (IBM Corporation, Armonk, NY, USA). Data were expressed as mean \pm standard deviation. Bland-Altman analysis was used to determine the concordance between EB-OCT measurements and histological findings. Differences in airway wall thickness between EB-OCT and histological measurement were tested with Student's *t* test or one-way analysis of variance. Paired *t* tests were conducted to determine the differences of EB-OCT parameters (airway wall thickness and gray-scale value) before and after modeling. Statistical significance was defined as $p < 0.05$ unless otherwise stated.

Results

Concordance between EB-OCT and Histological Analysis

There was no significant difference in airway wall thickness measured by EB-OCT and histology (95% confidence interval [CI] of the difference was -0.01 to 0.03 , $t = 1.58$, $p < 0.05$). The airway wall thickness assessed by EB-OCT had notable correlation with that measured by histology ($r = 0.957$, $p < 0.01$). The Bland-Altman plot showed that the majority of scattering dots were located

Fig. 1. Bland-Altman analysis of the airway wall thickness measured by EB-OCT and histology.

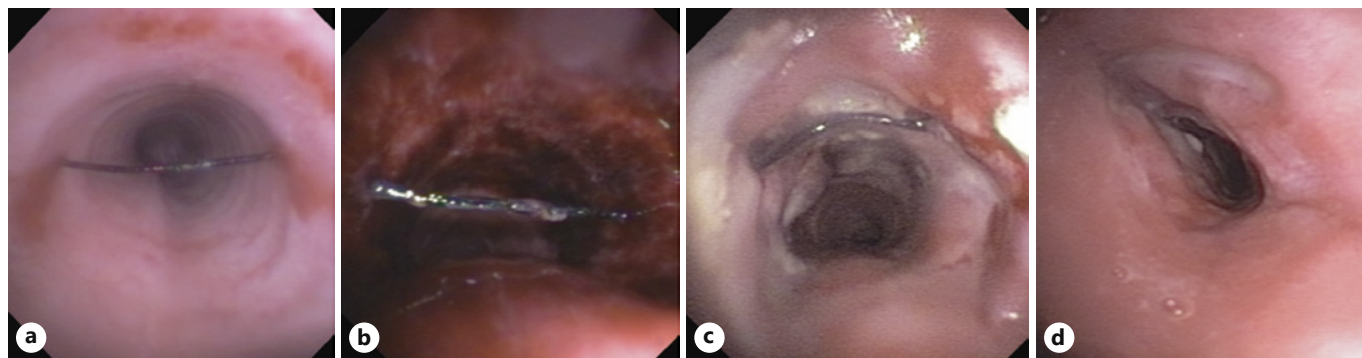
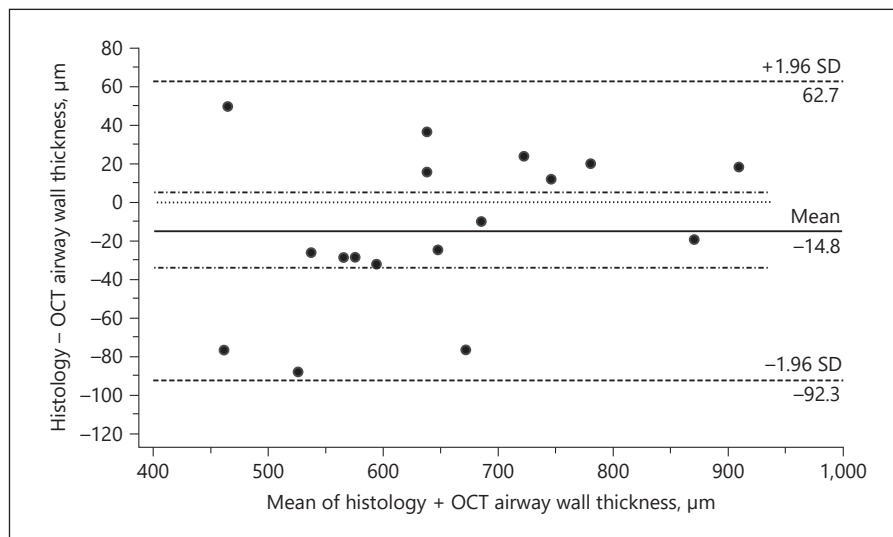


Fig. 2. Bronchoscopic findings during the development of PITS. **a** Tracheal lumen before intubation (the nylon wire was inserted for positioning). **b** Tracheal mucosal ischemic necrosis on the 1st day after modeling. **c** Edema, necrotic tissue, and granulation proliferation on the 7th day after modeling. **d** Hyperplastic granulation tissue and tracheal stenosis formation on the 12th day after modeling.

in the 95% CI, indicating a high concordance of airway wall thickness measured by EB-OCT and histology (Fig. 1).

Airway Structural Observation by Bronchoscopy and EB-OCT Examination

On the 1st day after extubation, the tracheal congestion and edema were observed under bronchoscopy. The proliferation of granulation tissue and mucosal edema, which led to moderate tracheal stenosis, was found at 1 week after modeling. On the 12th day after extubation, severe airway obstruction was developed by granulation hyperplasia and cicatrization (Fig. 2a–d).

The average airway wall thickness of normal segment measured by EB-OCT in 9 beagles was $363 \pm 58 \mu\text{m}$ and increased to $630 \pm 83 \mu\text{m}$ on the 1st day, $743 \pm 93 \mu\text{m}$ on

the 7th day, and $750 \pm 38 \mu\text{m}$ on the 12th day after extubation. The gray-scale value evaluated by EB-OCT was 117.09 ± 11.35 of the normal airways and decreased to 84.81 ± 9.17 on the 1st day, 80.73 ± 9.89 on the 7th day, and 83.00 ± 11.02 on the 12th day after modeling (Table 1).

The EB-OCT scanning provided a distinct picture of the epithelium, basement membrane, lamina propria, and cartilage of the normal airway wall (Fig. 3a). On the 1st day after extubation, the EB-OCT imaging (Fig. 3b) revealed an increase of airway wall thickness and attenuation of the OCT gray-scale value. Whilst the histopathological findings indicated that the neutrophil infiltration, vascular congestion, and tissue edema in the submucosal layer contributed to the thickening and heterogeneous density area of the airway wall based on OCT imaging

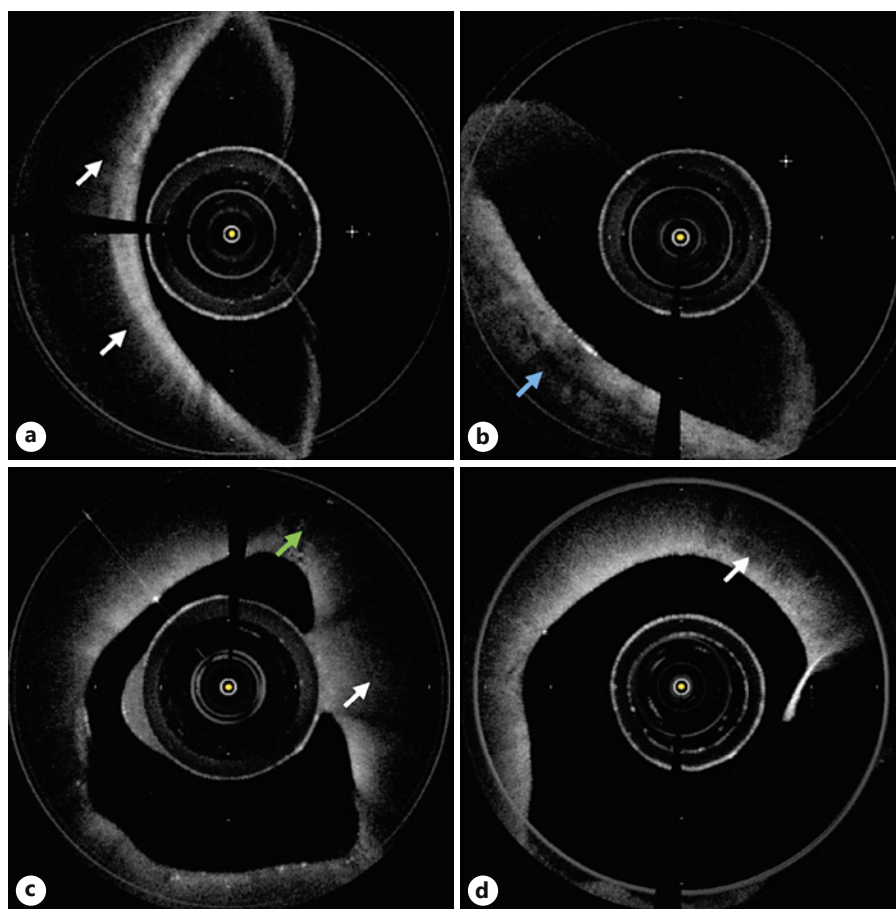


Fig. 3. EB-OCT images during the development of PITS. **a** Before modeling: mucosa, submucosa, and cartilage (white arrows) were well bedded. **b** Airway wall edema (blue arrow). **c** Granulation formation (green arrow) combined with cartilage damage (white arrow). **d** Airway wall thickening, cartilage destruction, and blurred airway wall layer (white arrow).

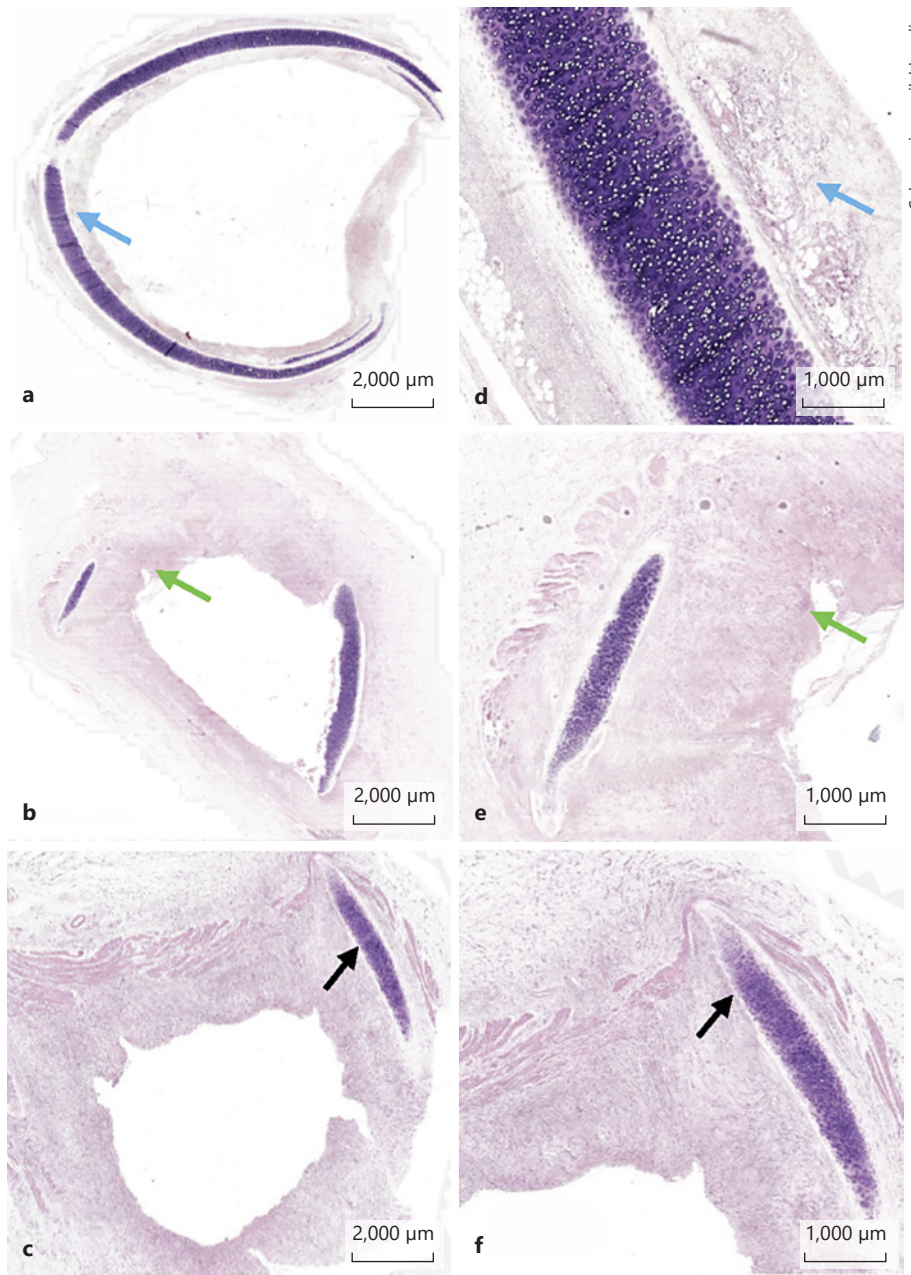
Table 1. EB-OCT measurement of airway morphology of PITS

	Before modeling*	1st day after modeling	7th day after modeling	12th day after modeling
Histological findings	–	neutrophil infiltration, vascular congestion, and edema	granulation proliferation and neovascularization	tracheal cartilage destruction and fibroblast hyperplasia
Airway wall thickness	363±58 μm	630±83 μm^{a}	743±93 $\mu\text{m}^{\text{a, b}}$	750±38 μm
Gray-scale value	111.19±14.71	85.68±8.48 ^a	79.06±9.10 ^{a, b}	83.00±11.02

^a $p < 0.05$, compared to that before modeling; ^b $p < 0.05$, compared to that on 1st day after modeling.

(Fig. 4a, d). On the 7th day after modeling, the airway wall was characterized by significant thickening and decreased in OCT gray-scale value (Fig. 3c), which was in line with histopathological findings (Fig. 4b, e) of granulation proliferation, neovascularization, and submucosal edema in the airway wall. Furthermore, the outer layer of the airway wall was not completely undamaged on the 12th day

after modeling, while the airway wall presented more thickening and progressive decrease of gray-scale value (Fig. 3d). Correspondingly, the tracheal histopathological examination (Fig. 4c, f) demonstrated airway cartilage destruction, granulation proliferation, as well as fibroblasts hyperplasia.



Color version available online

Fig. 4. Histological findings during the development of PITS. **a, d** Tissue edema (blue arrow) in the submucosal layer. **b, e** Granulation proliferation (green arrow), neovascularization, submucosal edema, and cartilage damage. **c, f** Tracheal cartilage destruction (black arrow), granulation proliferation, and fibroblast hyperplasia.

Consecutive EB-OCT Observation of Airway Structure during the Development of PITS

EB-OCT examination was performed daily in 3 canines from the 1st to the 9th day after modeling, since 2 of them suffered from dyspnea and were euthanized on the 9th day. Airway wall edema was found instantly after extubation and peaked on the 7th day, along with the loss of the mucosal boundaries. Granulation tissue developed at the mucosal layer of the airway wall from the 7th day

after modeling. The airway cartilage destruction was detected with EB-OCT on the 9th day. The thickness of the tracheal wall increased from $344.41 \pm 44.19 \mu\text{m}$ before modeling to $796.67 \pm 49.75 \mu\text{m}$ on the 9th day after modeling ($p < 0.05$). Intriguingly, the gray-scale values assessed by EB-OCT decreased from 111.19 ± 14.71 before modeling to 74.96 ± 4.08 on the 9th day after modeling ($p < 0.05$) (Fig. 5b), which had negative correlation with the airway wall thickness ($r = -0.945, p = 0.001$) (Fig. 5a).

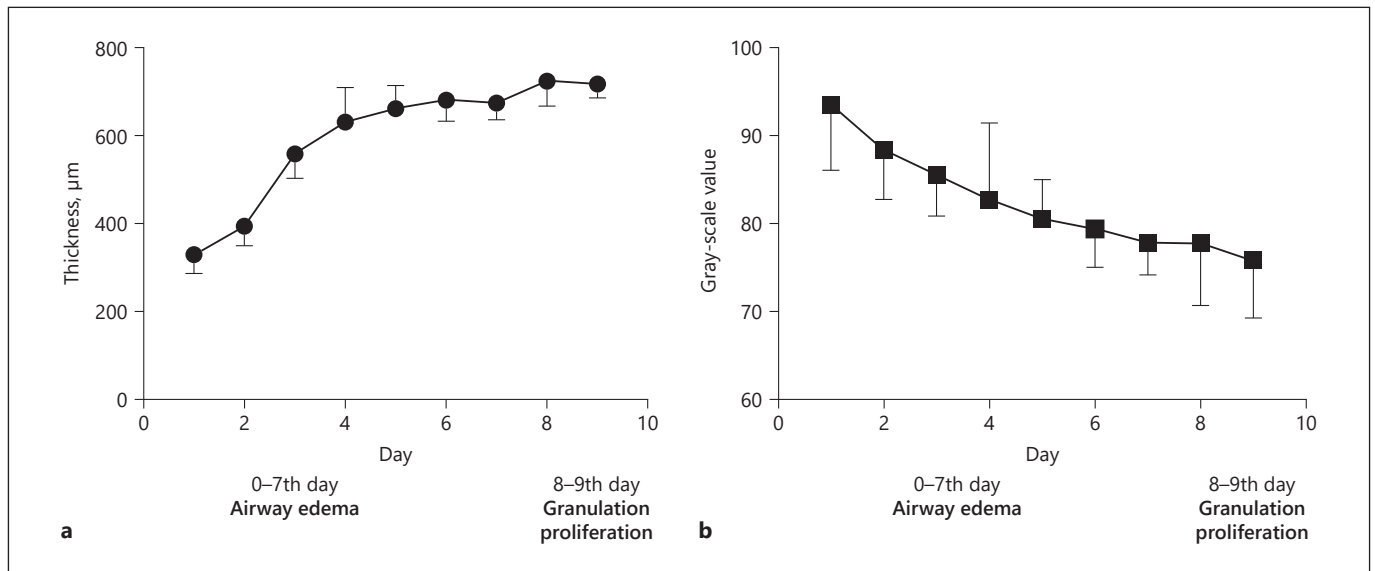


Fig. 5. a Airway wall thickness increased within 5 days. **b** The gray-scale value decreased since the first day after extubation.

EB-OCT Images Revealed the Development of PITS

EB-OCT imaging might help identify granulation hyperplasia, cartilage destruction, and fibroblast hyperplasia during the development of PITS. The dark areas presented in the airway wall with low gray-scale value on the 7th day after modeling indicated granulation tissue hyperplasia, which was verified by histopathology. Cartilage destruction and fibroblast hyperplasia were detected on the 9th day after modeling, presented as thickening and disintegration of the airway wall with low gray-scale value assessed by EB-OCT. Furthermore, the receiver operating curve (ROC) analysis of gray-scale value was performed to differentiate edema and granulation, indicating that the cut-off level of gray-scale value ≤ 81.35 conferred a sensitivity of 70.6% and a specificity of 72.2% to predict the development of granulation in the airway wall ($AUC^{ROC} = 0.765$; 95% CI, 0.692–0.839, $p < 0.001$) (Fig. 6).

Discussion

In the current study, we performed EB-OCT to demonstrate the airway structural changes after overinflated intubation in a beagle model. The EB-OCT imaging revealed the airway edema, granulation tissue proliferation, cartilage destruction, as well as airway wall thickness increased and gray-scale value attenuated during the development of PITS, which had a high concordance with the histopathological findings. Hence, EB-OCT could serve

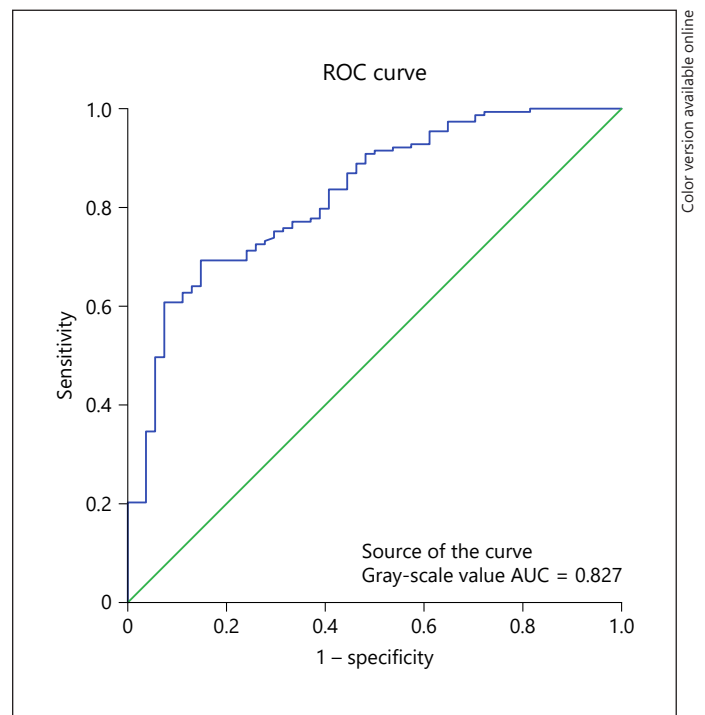


Fig. 6. The diagnostic performance of gray-scale value assessed by EB-OCT in discriminating granulation from edema in the airway wall. The receiver operating curve (ROC) analysis indicated that the cut-off level of gray-scale value ≤ 81.35 conferred a sensitivity of 70.6% and a specificity of 72.2% to present the development of granulation in the airway wall.

to consecutively observe and accurately measure the airway morphological abnormalities *in vivo*, which might help further understand the physiopathological mechanism of PITS.

EB-OCT provides a high-resolution imaging of the airway morphology and has reasonable correlation with CT scans and histopathological findings [9]. Coxson et al. [10] found a strong correlation between CT airway parameters and those assessed by OCT imaging, indicating a greater sensitivity of OCT in detecting the changes of airway wall measurements than CT. Ajose-Popoola et al. [11] used OCT to evaluate the injury segment of the trachea after intubation in a rabbit model, revealing that the OCT imaging of the airway edematous tissue correlated well with the pathological findings. The previous studies mentioned above revealed the validity of EB-OCT in accurately evaluating the airway morphology.

The type and degree of airway stenosis could be identified with bronchoscopy. However, the evaluation of submucosal lesion and cartilaginous damage, which contribute to the critical influences on the prognosis and therapeutic strategy, has been a clinical challenge. The OCT frequency, commonly set to 1,050 nm, appears to be an optimal value balance between light transmittance, scattering, and resolution for differentiating airway wall structural morphology [5, 12]. The point-by-point comparison between EB-OCT images and pathological findings showed that EB-OCT could distinctly display the morphological abnormalities of the mucosal and submucosal layers and airway cartilage. The mucosal and submucosal layers were visualized in off-white, indicating the relatively high optical backscattering, whereas the cartilage and granulation tissue were differentiated as the dark area with low optical scattering.

The excessive cuff pressure compression might lead to ischemic injury of the airway wall, or even tracheal stenosis [13, 14]. The local impairment of the mucosal or submucosal layers could cause normal wound healing. However, the damage of tracheal cartilage might induce proliferation rather than regeneration, which contributes to the key factor for tracheal stenosis, and commonly predicts the poor prognosis [15–17]. Cavaliere et al. [18] reported that the most important factor in predicting the outcome of endoscopic dilation for PITS was the grade of cartilaginous involvement, and concluded that evaluating the degree of granulation/scar formation and cartilage involvement could improve the outcome of endoscopic treatment. In the current EB-OCT study, we found that OCT imaging correlated well with the pathological findings, making it reasonable to distinguish the pathophysiological

changes during the development of PITS. Airway wall edema and granulation tissue hyperplasia could be identified by EB-OCT within a week after modeling. Moreover, the cartilage destruction, characterized by structural discontinuity, could be assessed on the 9th–12th days, which were in line with the characteristic of histological changes in the development of PITS [3]. Since the symptom of dyspnea in PITS commonly lags behind the granulation formation and cartilage damage, we believe that EB-OCT could play a role in evaluating and predicting the development of PITS.

The EB-OCT imaging reported to demonstrate the tissue water content had negative correlation with the OCT gray-scale value [19]. Since the OCT spectrum has minimum absorption of water [20], the hydration gradient would provide a greater backscattered light density, with greater hydration inducing more backscatter [19] and a lower gray-scale value. In the current study, the airway wall thickness had a negative correlation with the gray-scale value assessed by EB-OCT since the airway edema and granulation hyperplasia, presented with the increase of water content and a lower gray-scale value in EB-OCT, commonly contributed to the airway wall thickening in PITS. The gray-scale value decreased from the first day after extubation and maintained a low value after the 9th day, which was coincident with the pathological findings of inflammation and edema followed by the granulation tissue (consisting of higher water content) protruding into the tracheal lumen within 2 weeks, and fibroblast hyperplasia formation on the 12th day. Briefly, the gray-scale value evaluation obtained from EB-OCT measurement might help with further identification of airway wall components in PITS.

Some limitations should be taken into consideration in this study. First, 2 of 3 canines were sacrificed on the 9th day due to dyspnea caused by tracheal stenosis; hence, the long-term observation by EB-OCT in these 3 beagles was lacking. Second, due to the inner diameter of the tracheal lumen (approximately 1.6–1.8 cm in diameter), we could not perform complete circular scanning by using EB-OCT. Instead, we chose three scanning points at the anterolateral and bilateral wall to reveal the morphological features of the trachea. Third, as a limitation of scanning depth and resolution, some microstructures, including glands, capillaries, and fibrous tissue, could not be accurately identified and measured in this study.

In conclusion, EB-OCT imaging, in concordance with the histopathological finding, was validated for assessing the airway morphological changes during the development of PITS. EB-OCT evaluation of cartilage damage

and gray-scale value measurement might contribute to discriminate the airway wall composition, help illuminate the pathophysiological mechanism, and predict the development and prognosis of PITS.

Acknowledgments

We thank Guangzhou Winstar Medical Technology Company, who supported us with the technical operation of the OCTICS Imaging System.

Statement of Ethics

This animal study was approved by the Ethics Committee of Guangdong Medical Experimental Animal Center (Ethics No. 201710-5). All procedures were in line with the experimental animal processing of Guangdong Medical Laboratory Animal Center Regulations.

Disclosure Statement

The authors have no conflicts of interest to declare.

References

- 1 Kreienbühl G. [Tracheal stenosis following prolonged nasotracheal intubation with a plastic tube and prestretched cuff]. *Anaesthesist*. 1973 May;22(5):243–4. German.
- 2 Miller DR, Sethi G. Tracheal stenosis following prolonged cuffed intubation: cause and prevention. *Ann Surg*. 1970 Feb;171(2):283–93.
- 3 Su Z, Li S, Zhou Z, Chen X, Gu Y, Chen Y, et al. A canine model of tracheal stenosis induced by cuffed endotracheal intubation. *Sci Rep*. 2017 Mar;7(1):45357.
- 4 Freitag L, Ernst A, Unger M, Kovitz K, Marquette CH. A proposed classification system of central airway stenosis. *Eur Respir J*. 2007 Jul;30(1):7–12.
- 5 Han S, El-Abadi NH, Hanna N, Mahmood U, Mina-Araghi R, Jung WG, et al. Evaluation of tracheal imaging by optical coherence tomography. *Respiration*. 2005 Sep-Oct;72(5):537–41.
- 6 Lam S, Standish B, Baldwin C, McWilliams A, leRiche J, Gazdar A, et al. In vivo optical coherence tomography imaging of preinvasive bronchial lesions. *Clin Cancer Res*. 2008 Apr;14(7):2006–11.
- 7 Tsuboi M, Hayashi A, Ikeda N, Honda H, Kato Y, Ichinose S, et al. Optical coherence tomography in the diagnosis of bronchial lesions. *Lung Cancer*. 2005 Sep;49(3):387–94.
- 8 Huang D, Swanson EA, Lin CP, Schuman JS, Stinson WG, Chang W, et al. Optical coherence tomography. *Science*. 1991 Nov;254(5035):1178–81.
- 9 Chen Y, Ding M, Guan WJ, Wang W, Luo WZ, Zhong CH, et al. Validation of human small airway measurements using endobronchial optical coherence tomography. *Respir Med*. 2015 Nov;109(11):1446–53.
- 10 Coxson HO, Quiney B, Sin DD, Xing L, McWilliams AM, Mayo JR, et al. Airway wall thickness assessed using computed tomography and optical coherence tomography. *Am J Respir Crit Care Med*. 2008 Jun;177(11):1201–6.
- 11 Ajose-Popoola O, Su E, Hamamoto A, Wang A, Jing JC, Nguyen TD, et al. Diagnosis of subglottic stenosis in a rabbit model using long-range optical coherence tomography. *Laryngoscope*. 2017 Jan;127(1):64–9.
- 12 Fujimoto JG, Brezinski ME, Tearney GJ, Boppart SA, Bouma B, Hee MR, et al. Optical biopsy and imaging using optical coherence tomography. *Nat Med*. 1995 Sep;1(9):970–2.
- 13 Roscoe A, Kanellakos GW, McRae K, Slinger P. Pressures exerted by endobronchial devices. *Anesth Analg*. 2007 Mar;104(3):655–8.
- 14 Yousem SA, Dauber JH, Griffith BP. Bronchial cartilage alterations in lung transplantation. *Chest*. 1990 Nov;98(5):1121–4.
- 15 Marshak G, Doyle WJ, Bluestone CD. Canine model of subglottic stenosis secondary to prolonged endotracheal intubation. *Laryngoscope*. 1982 Jul;92(7 Pt 1):805–9.
- 16 Dohar JE, Klein EC, Betsch JL, Hebda PA. Acquired subglottic stenosis—depth and not extent of the insult is key. *Int J Pediatr Otorhinolaryngol*. 1998 Dec;46(3):159–70.
- 17 Zagalo C, Santiago N, Grande NR, Martins dos Santos J, Brito J, Aguas AP. Morphology of trachea in benign human tracheal stenosis: a clinicopathological study of 20 patients undergoing surgery. *Surg Radiol Anat*. 2002 Aug-Sep;24(3-4):160–8.
- 18 Cavaliere S, Bezzi M, Toninelli C, Foccoli P. Management of post-intubation tracheal stenoses using the endoscopic approach. *Monaldi Arch Chest Dis*. 2007 Jun;67(2):73–80.
- 19 Wang J, Simpson TL, Fonn D. Objective measurements of corneal light-backscatter during corneal swelling, by optical coherence tomography. *Invest Ophthalmol Vis Sci*. 2004 Oct;45(10):3493–8.
- 20 Schmitt JM, Knüttel A, Yadlowsky M, Eckhaus MA. Optical-coherence tomography of a dense tissue: statistics of attenuation and backscattering. *Phys Med Biol*. 1994 Oct;39(10):1705–20.

Funding Sources

Prof. Li declares that he received funding from the National Natural Science Foundation of China (No. 81770017) and Clinical Innovation Research Program of Guangzhou Regenerative Medicine and Health Guangdong Laboratory (No. 2018GZR0201002). Dr Su declares that he received funding from the National Natural Science Foundation of China (No. 81900032) and the Youth Fund of Sate Key Laboratory of Respiratory Disease (SKLRD-QN-201914). Dr Chen declares that he received funding from the Natural Science Foundation of Guangdong province (No. 2018A030310297). None of the funding sources had any role in the study.

Author Contributions

Z.-Q.Z., Z.-Q.S., W.S., M.-L.Z., Y.C., C.-H.Z., and H.-J.C. performed the literature search, drafted the manuscript, and were responsible for the establishment of the animal model. Z.-Q.Z., Z.-Q.S., and W.S. contributed to the EB-OCT performance, data collection, and data analysis and interpretation. Z.-Q.Z. and Z.-Q.S. performed the statistical analyses. Z.-Q.Z., Z.-Q.S., and S.-Y.L. contributed to the study conception. S.-Y.L. provided critical revision of the manuscript and approved the final submission.